



ANTI-CANCER ACTIVITY OF GREEN SYNTHESIZED SILVER AND GOLD NANOPARTICLES USING *OCHNA OBTUSATA* LEAF.

STELLA SRAVANTHI VALATHATI[§], HEMANTH NAICK^{||}, SRAVATHI[#] and P. LATHA^{§*}.

[§]Department of Biochemistry & Molecular Biology, School of Sciences, Pondicherry University, Puducherry-605014, India.

[#]Department of Sports & Science, School of Sports Science, Central University of Rajasthan, Rajasthan-305817, India.

*Corresponding author Email: paperiyasathil@gmail.com

In this study, we have employed green method for the synthesis of silver and gold metal nanoparticles through rapid single step method by using *Ochna obtusata* leaf extract as a reducing agent. Synthesized AgNP (Silver Nanoparticles) and AuNP (Gold Nanoparticles) were confirmed with SPR (Surface Plasmon Resonance) peak by UV-Vis spectroscopy. The resulting nanoparticles were characterized by employing DLS (Dynamic light scattering), FTIR (Fourier Transmission Infra-Red), XRD (X-Ray diffraction) and HRTEM (High-resolution transmission electron microscopy), EDX (Energy Dispersive X-ray spectroscopy), SAED (Selected Area Electron Diffraction), and Elemental mapping analysis. Resulting anticancer capabilities of AgNP and AuNP were evaluated against breast cancer cell lines. The results showed that biosynthesized AgNP and AuNP exhibited an absorption peak at 440nm and 540nm, respectively. Both SAED and XRD analysis has established the crystalline nature of silver and gold nanoparticles in face-centered cubic (FCC) structure. FTIR spectra have shown the involvement of plant compounds during the reduction of Ag⁺ and Au⁺ nanoparticles. The TEM images have displayed the spherical structure of AgNP, and an anisotropic structure for AuNP with an average diameter determined to be 26nm and 29nm respectively. Besides, both AgNP and AuNP have exhibited anticancer property against MDA-MB 231 and MCF-7 breast cancer cell lines. In conclusion, we have used *O. obtusata* for the first time as reducing as well as a capping agent for the synthesis of AgNPs and AuNPs and anticancer activity of AgNPs and AuNPs is established against breast cancer cells.

Keywords: Biosynthesis, *Ochna obtusata*, Metal nanoparticles, Green chemistry, Anticancer.

Introduction

In recent years, Nanoparticles has emerged as a promising tool in drug delivery and cancer therapy¹⁻⁴. Nanoparticles with 1-100nm size have received massive attention and played a crucial role in nanotechnology and nano-medicine due to its salient feature like the high surface area to volume ratio and making them easy to interact with other particles⁵⁻⁷.

Nanoparticles disclose unique properties like optical, catalytic, biological, magnetic and therapeutic applications etc⁸⁻¹¹. Nanoparticles were synthesized by employing different methods such as synthesis chemical, physical, and biological methods¹²⁻¹⁴. In which, the biological method has a promising effect due to rapid, eco-friendly, and low toxic properties¹⁵. Sources like bacteria, fungi,

algae, plants act as reducing agents in biogenic methods¹⁶⁻¹⁸. Silver nanoparticles synthesized through green method has potent inhibitory and anti-bacterial properties among other nanomaterial¹⁹⁻²¹. Numerous studies on both silver and gold nanoparticles have revealed their unique biological properties²²⁻²⁴ along with anti-proliferative and anti-apoptotic property in cancer therapy^{3,25,26}. Gold nanoparticles have also received a tremendous interest due to their vast applications in vaccine production as carriers, adjuvants, reducing toxicity, increasing immunogenic activity, and even in imaging, diagnostic etc²⁷⁻²⁹. Therefore, Green chemistry in nanomaterial synthesis has been increased significantly over other biological methods due to its simple, non-toxic, cost-effective, and eco-friendly process³⁰. Further, phytochemical constituents present in leaves, roots, bark, stem, flowers act as reducing as well as capping agents³¹. Flavonoids, a class of pigments are majorly involved in the reduction process of green method³².

O. obtusata is a tree with a woody stem and glossy leaves with attractive yellow flowers belongs to Ochnaceae family. *O. obtusata* is native of East India and commonly known as *Ramdhan champa*³³. There are 85 species of Ochna genus widely used as a traditional medicine in Asia, Africa, and America, among which 11 species occur in India³⁴. Plant parts like bark, leaves, and roots of *O. obtusata* were used in traditional medicine for treating several ailments like dysentery, asthma, diarrhoea, menstrual disorder, cholera, inflammation, bronchitis, and dysmenorrhoea^{35,36}. Based on the reported literature, the glossy leaves of *O. obtusata* contains bioactive compounds like flavonoids and bioflavonoids; quercetin 3-o-glucoside, kaempferol 3-o- β -glucoside, ochnaflavone, 2,3-dihydroochnaflavone 7-o-methyl ether, 2,3-dihydroochnaflavone³⁷.

In the present study, we approached green chemistry for

synthesizing both AgNps and AuNps using *O. obtusata* leaf aqueous extract (OLAE) as a reducing and stabilizing agent. So far to our knowledge, there is no reported synthesis of nanoparticles using *O. obtusata* as a bio-reductant. Biosynthesized AgNps and AuNps is characterized by energy dispersive X-ray Spectroscopy (EDX), Transmission electron microscopy (TEM), Selected Area Electron Diffraction (SAED), Fourier transform infrared spectroscopy (FTIR), Dynamic Light Scattering (DLS), X-Ray Powder Diffraction (XRD), and Elemental mapping analysis. Further, the anti-cancer property of synthesized nanoparticles were evaluated against breast cancer MDA-MB 231 and MCF-7 cell lines.

Material and methods

O. obtusata leaves were obtained from Tirupati, Andhra Pradesh. An analytical grade Silver nitrate (AgNO_3), Gold chloride trihydrate ($\text{HAuCl}_4 \cdot \text{H}_2\text{O}$) and MTT (3-(4, 5-Dimethylthiazol-2-yl)-2, 5-Diphenyltetrazolium Bromide) was purchased from Sigma-Aldrich (St. Louis, MO). Human adenocarcinoma breast cancer MDA-MB 231 and MCF-7 cell line were purchased from NCCS, Pune. All the aqueous solutions are prepared by using Milli-Q water.

Preparation of *O. obtusata* aqueous leaf extract:

Thoroughly washed and dried leaves of *O. obtusata* were coarsely ground and stored in an air tight container. The coarse powder of 1g was soaked overnight in 100ml of Milli-Q water. The solution was heated at 40°C under continuous stirring process for 5 min. The solution was filtered by using Whatman No-1 filter paper. Then, the Obtained filtrate was stored a week at 4°C for further experiments.

Synthesis and purification of AgNP and AuNP:

1mM concentration of AgNO_3 and $\text{HAuCl}_4 \cdot \text{H}_2\text{O}$ solution was prepared. For the synthesis of nanoparticles, we have used different volumes of *O. obtusata*

aqueous leaf extract (OAE) (0.5ml, 1ml, 2ml, 3ml, 4ml, 5ml) against constant metal ion concentration. An optimised ratio for the synthesis of AgNP was done by mixing 1ml of OAE with 9ml of AgNO₃, whereas AuNP were synthesised by mixing 3ml of OAE with 7ml of 1mM HAuCl₄.H₂O. The reaction mixture for both silver and gold nanoparticles were allowed to stir on a magnetic stirrer at 200rpm speed for 1 and 30 mins incubation at room temperature respectively. Reduction of Ag⁺ ions to Ag⁰ and Au⁺ to Au⁰ can be confirmed by the change of colour from pale yellow to dark brown colour and purple colour respectively. Further confirmation of AgNP and AuNP synthesis was done by measuring absorption spectra at a range of 300-700nm at regular intervals using UV-visible spectroscopy. Following incubation, the reaction mixture of AgNP and AuNP were subjected to centrifugation at 12000 rpm for 30 mins each by repeated washes with Milli-Q water. The washed pellet was dried and preserved for further characterisation.

Characterisation of AgNps and AuNps:

The unique optical property of silver nanoparticles was measured by the absorption spectrum at a range 200-700nm using UV-visible spectroscopy (UV-VIS-spectrophotometer; Varian Model: 5000). An average hydrodynamic size and Poly Dispersive Index (PDI) of AgNP and AuNP were determined by using particle size analyser zetaser (MALVERN instruments Nano ZS) at 24.9°C. Bio-reduction of silver nitrate by the functional groups present in the leaf extract can be identified by using FTIR measurements (Thermo Nicolet Model:6700 equipped with KBr optics) with the wave number range 5000-700 cm⁻¹ at resolution 0.1cm⁻¹. Surface morphology, size, elemental composition and elemental distribution of AgNP and AuNP were determined by using HRTEM, EDX and elemental mapping analysis operated with an instrument (TEM TECNAI-G2 F30-F TWIN) at 200kV. Preparation of sample for

TEM analysis was done by dropping 5µl of ethanol dispersed AgNP and AuNP on a carbon coated copper grid and allowed to dry under vacuum. The crystalline structure of silver and gold nanoparticles was analysed by the SAED and XRD patterns. XRD records by using XRD (PAN analytical) with the step size 0.02° operated with CuKα, at settings 30 mA, 40kV, over 2θ range from 20°-80°. The size of both AgNP and AuNP was calculated using the Debye-Scherrer equation.

In-vitro anti-cancer activity of AgNP and AuNP

Cell culture conditions:

Cancer cell lines MDA MB-231, MCF-7 (human breast adenocarcinoma epithelial cells) were cultured in Dulbecco's Modified Eagle Medium (DMEM) with 1000mg/L glucose, L-glutamine and sodium bicarbonate which is supplemented with 10% FBS, 1% Penicillin (100U/ml) and streptomycin (100ug/ml). Cultured cells were incubated under 5% CO₂ at 37°C until it reaches 80% confluence.

MTT assay:

Cytotoxicity evaluation of synthesised AgNP and AuNP was performed by using MTT (3-(4, 5-Dimethylthiazol-2-yl)-2, 5-Diphenyltetrazolium Bromide) assay as previously reported protocol³⁸. All the experiments were done in triplicates. Cell viability and 50 % growth inhibition (IC₅₀) were determined and calculated by the following equation.

$$\% \text{ of cell inhibition} = 100 - [(At-Ab) / (Ac-Ab)] \times 100$$

$$\% \text{ of cell viability} = [(At-Ab) / (Ac-Ab)] \times 100$$

DNA Fragmentation assay:

DNA fragmentation is largely considered as a distinctive feature of apoptosis³⁹. DNA fragmentation assay is performed as described by Hackenberg, S. et al. 2011⁴⁰, with slight modifications. MCF7 (1*10⁶ cells/mL) were seeded in 6-well microplates and treated with increasing concentration 5, 10 and 15µg/mL of AgNP and AuNP respectively

for 24h. Following cells were collected and DNA is isolated by using DNeasy blood and tissue kit (Qiagen). The resultant DNA was quantified using nanodrop. For Estimating the DNA fragmentation equal amounts of DNA is loaded and run on 1.0% agarose gel containing 1 µg/mL ethidium bromide at 90 V for 1.5 h in 1 × TAE buffer of pH 8.5. Later the DNA fragments were visualized by exposing the gel to ultraviolet light, followed by photography.

Results and discussion

Synthesis of AgNP and AuNPs:

In this study for the first time, we are reporting biosynthesis of AgNPs and AuNPs by utilising aqueous extract of *O. obtusata* as a reducing agent in rapid single pot green synthesis approach. An overview work plan of silver and gold nanoparticles synthesis represented in (fig: 1 (i)). Both silver and gold nanoparticles synthesis was observed and confirmed by the colour change of reaction mixture to dark brown and purple colour respectively due to Surface Plasmon Resonance (SPR)⁴².

Investigation of results has revealed that *O. obtusata* aqueous leaf extract act as a reducing agent as well as stabilising agent for the synthesis of AgNPs and AuNPs. Synthesis of AgNP and AuNP was confirmed within 6 hrs and 30 min respectively, with a colour change from pale yellow to dark brown and purple respectively. Reduction of Ag^+ ions to Ag^0 (AgNPs) and Au^+ to AuNPs were confirmed by using U.V visible spectroscopy. Surface plasmon resonance (SPR) absorption band^{42,43} is observed at 440nm for AgNPs and 540nm for AuNPs (fig: 1, (II) (a) and (III) (a)). Time dependent synthesis of AgNPs and AuNPs were recorded using measuring SPR absorption band as shown in UV-VIS spectra in fig:1 (fig:1, (II) (b) and (III) (b)). The intensity and broadening of SPR band was increased constantly by the increase of reaction time due to the

increase in the concentration of nanoparticles.

Characterisation of AgNP and AuNPs:

DLS:

The average hydrodynamic size of AgNP and AuNP measured was 86.79nm and 112nm respectively which is based on scattering of light in DLS particle analysis. The PDI (Polydispersity Index) value of AgNP and AuNP was 0.346% and 0.29% respectively which represents monodispersed preparation and acceptable for drug delivery applications⁴⁵. The particle size distribution intensity of synthesised Gold and Silver was shown in (fig: 1 (ii); (a) and (b)).

TEM, EDX and Elemental mapping analysis:

Synthesised AgNP and AuNP were observed under TEM for visualizing their size and morphology. Results interestingly revealed that gold nanoparticles show anisotropic shape like hexagonal, triangular, rod and spherical particles with an average diameter ranging 26nm (figure: 2 (I); (a)). Whereas, silver nanoparticles have shown spherical shape with an average diameter ranging 28nm (figure: 2 (I); (b)). Besides AgNP and AuNP have shown uniform and monodispersed in nature respectively.

The crystallinity and the elemental distribution inside the AgNP and AuNP nanoparticles were analysed in more detail by energy dispersive X-ray spectroscopy. A characteristic sharp absorption peaks for AgNP (fig:2 (II); (a)) and AuNP (fig:2 (II); (b)) at 3keV and 2.5keV was observed respectively in EDX spectrum as shown in fig:2 (II); (a & b), which is a typical energy value for metallic silver and gold nanocrystallites⁴⁶. Additional peaks of carbon and oxygen were also present confirming the successful capping of *O. obtusata* plant compounds on the surface of AgNP and AuNPs. Furthermore, absorption peak for copper is also observed due to the usage of carbon-coated copper grid for the study⁴⁷. Further, an elemental mapping analysis of AgNP and AuNP were carried out to know

the distribution of respective nanoparticles. fig: 2 (III); (a, b & c) shows the selected electron micrograph region of synthesised silver nanoparticles and their distribution, corresponding fig: 2 (III); (d, e & f) shows the selected area and distribution of respective gold nanoparticles. Based on the

distribution shown in the figure we can confirm the purity of synthesised silver and gold nanoparticles due to their predominant over the corresponding products⁴⁸.

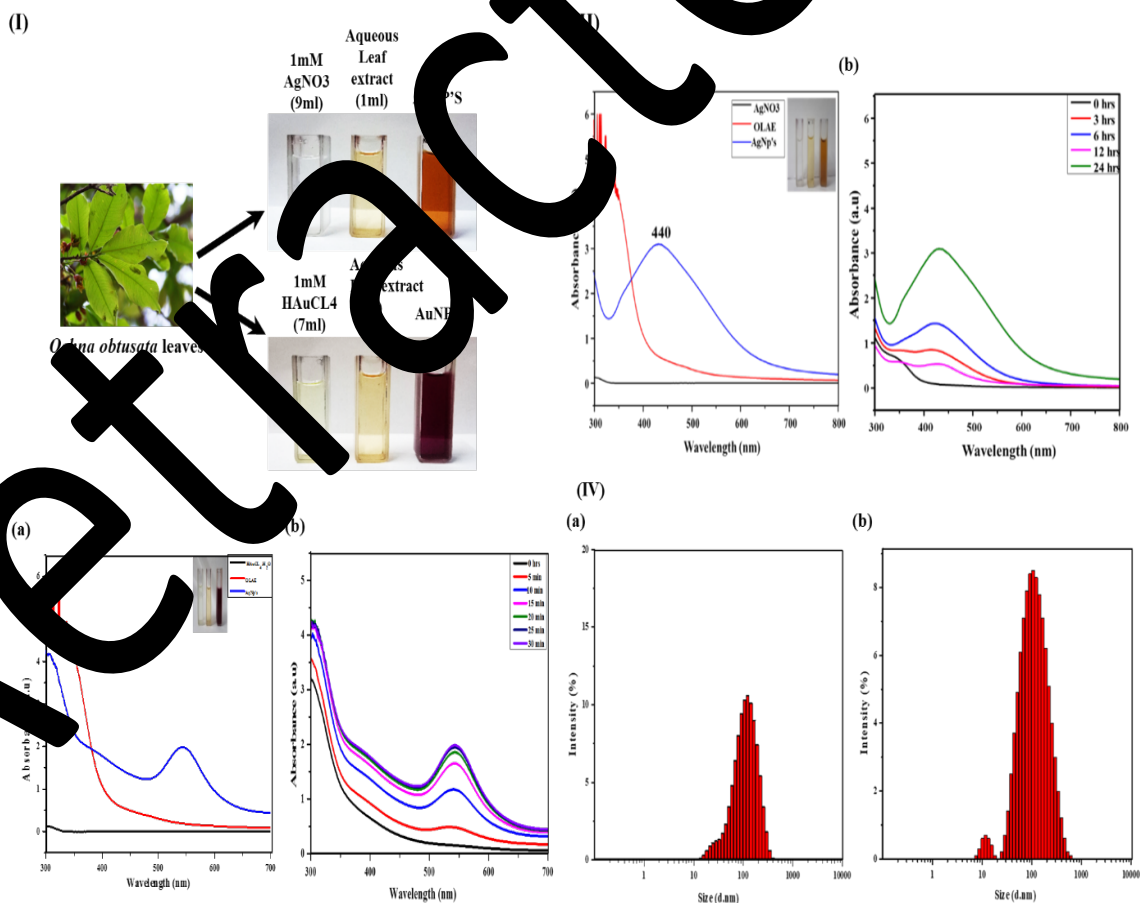


Figure 1:

- (I) Schematic synthesis of Silver and Gold nanoparticles using *O. obtusata* Aqueous leaf extract
- (II) (a) U.V-Vis spectra of AgNO₃ Solution, *O. obtusata* aqueous leaf extract (OAE) and silver nanoparticles (b) Time dependant analysis of silver nanoparticles (AgNP'S) prepared by 9ml of 1mM silver nitrate solution and 1ml of plant extract
- (III) (a) U.V-Vis spectra of HAuCl₄.H₂O Solution, *O. obtusata* aqueous leaf extract (OAE) and gold nanoparticles (b) Time dependant analysis of Gold nanoparticles (AuNP'S) prepared by 7ml of 1mM silver nitrate solution and 3ml of plant extract.
- (IV) Size distribution by intensity of (a) Gold nanoparticles and (b) Silver nanoparticles.

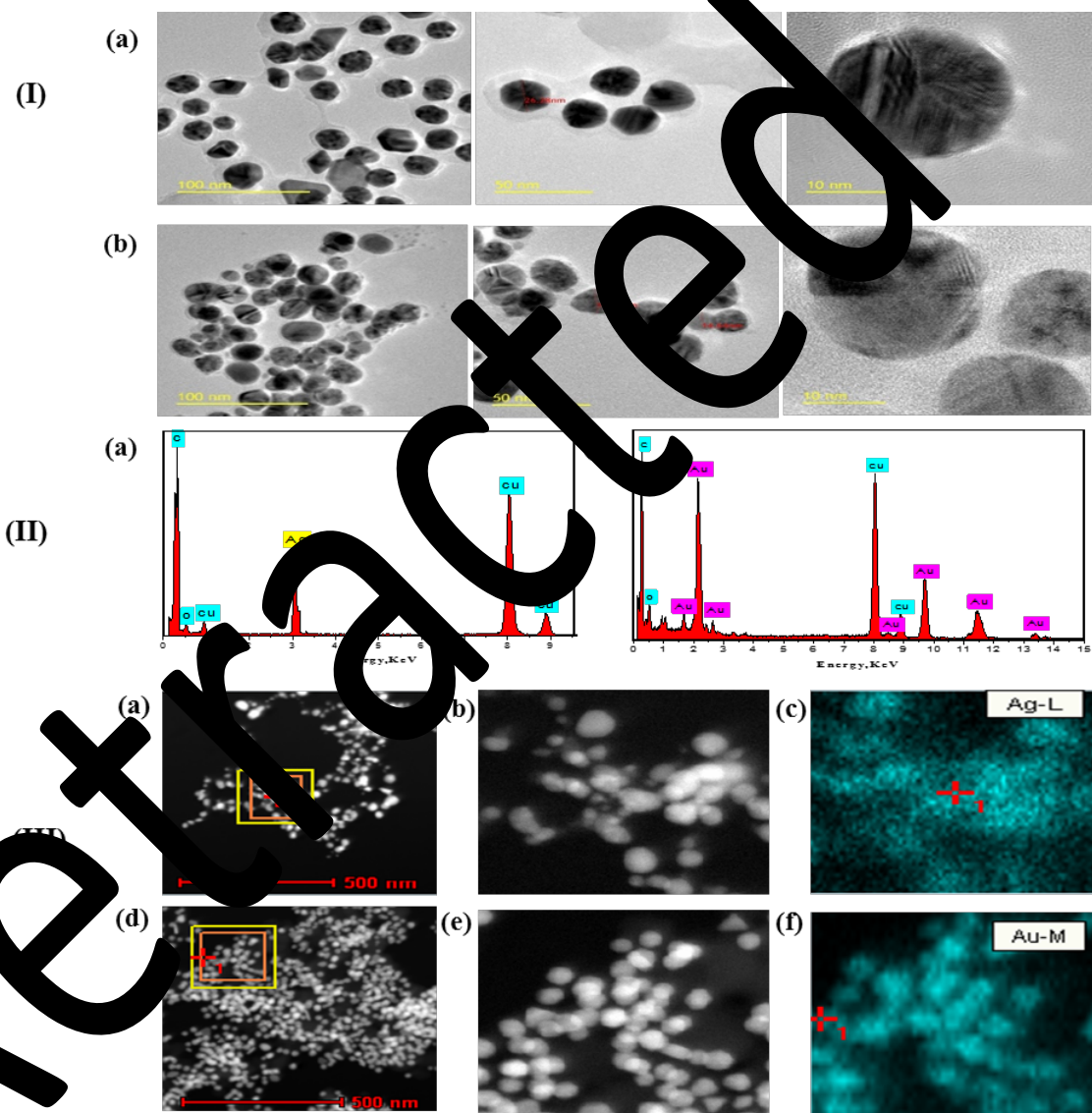


Figure 2:

(I) High-Resolution Transmission Electron Microscopy (HRTEM) images of biosynthesised gold (a) and silver (b) nanoparticles at 100nm, 50nm and 10 nm resolution.

(II) EDX spectra of silver (a) and gold (b) nanoparticles.

(III) Selected area elemental mapping results indicate the distribution of elements, the TEM micrograph of silver nanoparticle pellet solution (a, b), and silver element; blue (c) respectively. TEM micrograph of gold nanoparticle pellet solution (d, e), and gold element; blue (f) respectively.

FTIR, XRD spectra and SAED pattern:

FTIR spectra of *O. obtusata*, AgNP, and AuNP was shown in fig:3 (I) revealing the functional groups involved in reduction and stabilisation. The IR spectra of *O.obtusata* showed a wide range absorption peaks around 3407,2919, 2851, 1521,1284,1064,589 cm^{-1} assigned to O-H, C-O, C-H, C=C, S=O and C-Br which are

vibrational-stretching of alcohols, phenols, tertiary amines, alkanes, and alkenes respectively⁴⁹. The IR spectra of AgNP has displayed a prominent absorption peak at 3409 cm^{-1} corresponding to O-H stretching and peaks at 1611,1526,1441,1270 cm^{-1} indicates the involvement of flavonoids, phenols, alkanes, and alkenes in the reduction of

silver nitrate. Whereas IR spectra of AuNP showed an intense peak at 3397 cm^{-1} assigned to O-H stretching and 1610,1513,1441,1283,514 cm^{-1} assigned to C=C, N-O,C-H.C-O,C-Br vibrational stretching respectively indicating the involvement of alkanes, alkenes, amines, alcohols, and halo compounds during reduction. Herewith the IR spectra show that *O. obtusata* leaf extract acts as reducing as well as capping agent during silver and gold nanoparticle synthesis. Powder XRD pattern of AgNP and AuNP was shown in fig:3 (ii); (a,b). Obtained diffraction peaks of AgNP and AuNP at 2 θ degrees values of 37.92 $^\circ$, 44.05 $^\circ$, 44.6 $^\circ$

corresponds to (111),(200) (220) facets of face centred cubic (FCC) crystal lattice structure which is matched with earlier reported green synthesis method⁴⁷. The calculated crystal structure of AgNP and AuNP are 10.5nm and 10.2nm size respectively obtained by using following Debye-Scherrer's

$$\text{Crystallite size } D = \frac{K \times \lambda}{\beta \times \cos\theta}$$

Where D indicates the mean crystallite size, K is a scherrers constant (K=0.94), λ is X-ray wavelength, β is full width at half maximal (FWHM) intensity, θ is Bragg angle.

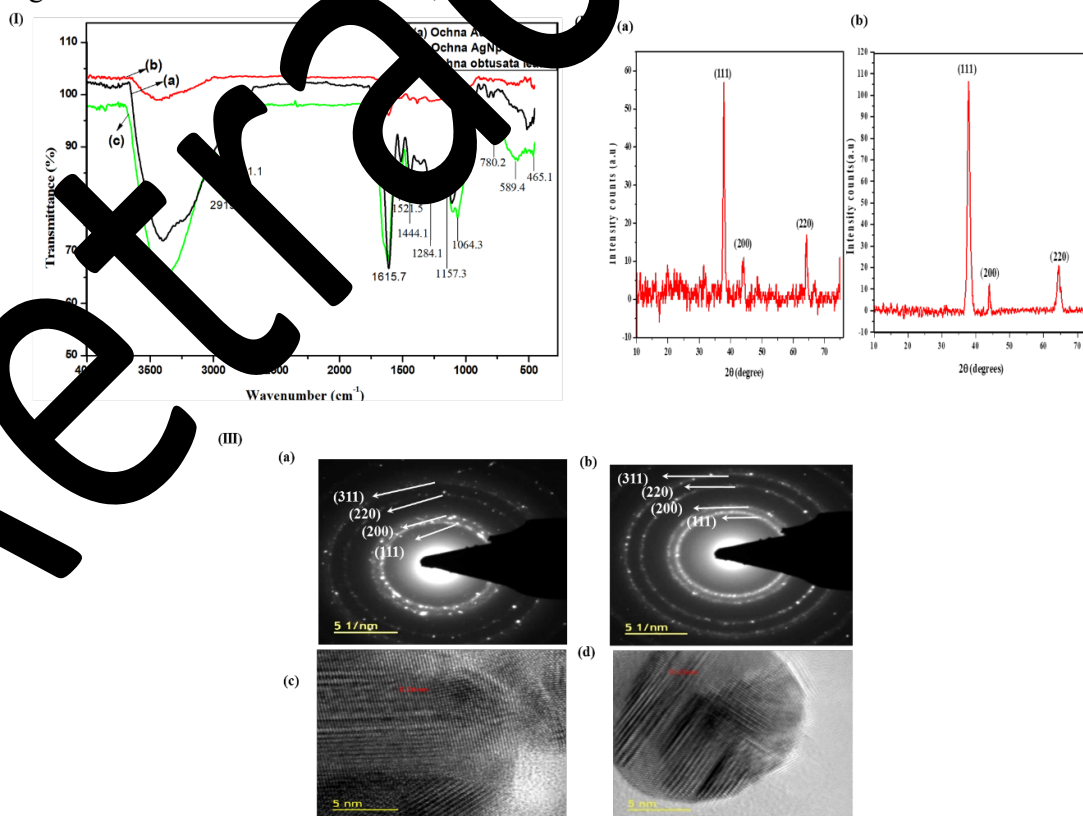


Figure: 3 (i) FTIR spectra of *O. obtusata* leaf extract and silver and gold nanoparticles. (ii) (a & b) indicates XRD spectra of silver (a) and gold nanoparticles (b). (iii) SAED pattern of silver (a) and gold (b) nanoparticles where the four circular rings assigning to (111), (200), (220), and (311) characterise the face centered cubic structure which was further proved with a lattice fringe spacing in fig:3 (iii);(c & d) with the distance of 0.26nm and 0.23nm obtained from high resolution transmission electron micrograph (HRTEM). Through the results obtained from XRD, SAED and HRTEM micrograph images, the synthesised silver and gold metal nanoparticles from *O. obtusata* are crystalline in nature.

Anti-cancer activity of AgNP and AuNPs:

In-vitro cytotoxicity of AuNP and AgNP against MCF-7 and MDA-MB-231 cells were measured using MTT colorimetric assay after 48h incubation.

Results of MTT assay were shown in fig: 4, untreated cells were considered as control. In agreement with other studies⁵⁰⁻⁵², our synthesised nanoparticles showed significant cytotoxicity compared to the

untreated population. The calculated IC_{50} values of AuNP against MCF-7 and MDA-MB-231 is $20.059\mu\text{g/ml}$ and $19.016\mu\text{g/ml}$ respectively. Whereas the AgNP IC_{50} values are 18.047 and 16.80 against MCF-7 and MDA-MB-231 cell lines respectively. The plant extract alone has shown minimal cytotoxicity when compared to synthesised nanoparticles.

The cytotoxicity of AuNP and AgNP is more towards MDA-MB-231 cells than MCF-7 cells. The cytotoxicity of synthesised NPs was significantly high when compared to Plant extract. This increase in cytotoxicity of synthesised nanoparticles may be due to increase in cellular uptake and retention of NP's in cells.⁵³

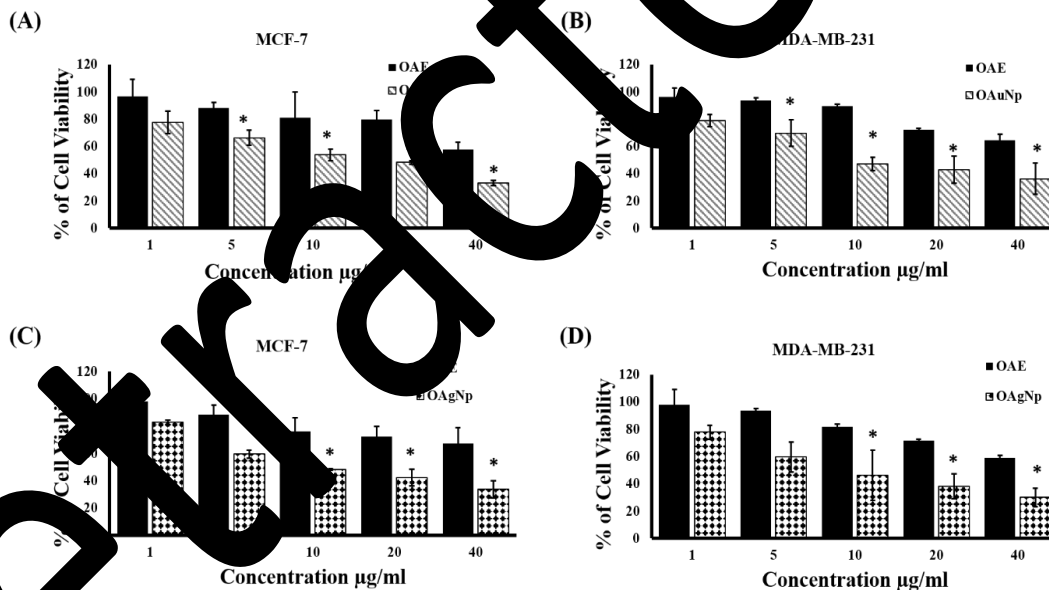


Figure: 4 Dose dependent in-vitro Cytotoxicity assay of Gold nanoparticles (A, B) and silver nanoparticles (C, D).

DNA Fragmentation assay:

Apoptosis inducing capabilities of synthesised AgNP and AuNP were verified by DNA laddering assay. The results revealed that AgNP and AuNP have induced inter nucleosomal DNA fragmentation in MCF7 cells with increasing concentration of nanoparticles (fig 5), DNA fragmentation is the characteristic feature of apoptosis induction. When compared to the control cells (untreated) the extent of DNA fragmentation caused by AgNP is prominent with increasing concentration. Control cells have shown minimum breakage of DNA, whereas at $15\mu\text{g/ml}$ of AgNP and AuNP has exhibited there by extensive double strand breaks, thereby yielding a ladder appearance (fig 5).

Conclusion:

The leaf extract of *O. obtusata* acts as a reducing agent as well as stabilising agent for the synthesis of Silver and Gold nanoparticles. An eco-friendly and fast facile synthesis of AgNPs and AuNPs by *O. obtusata* leaf extract were done. Synthesised AgNP and AuNP are stable for 2 months without the involvement of any hazardous chemicals further characterisation was done by FTIR, TEM, DLS, SAED, XRD, and elemental mapping analysis. Our anti-cancer activity assay revealed that AuNP and AgNP'S had exhibited significantly high toxicity towards breast cancer cell lines MDA-MB-231 and MCF -7 than plant extract alone.

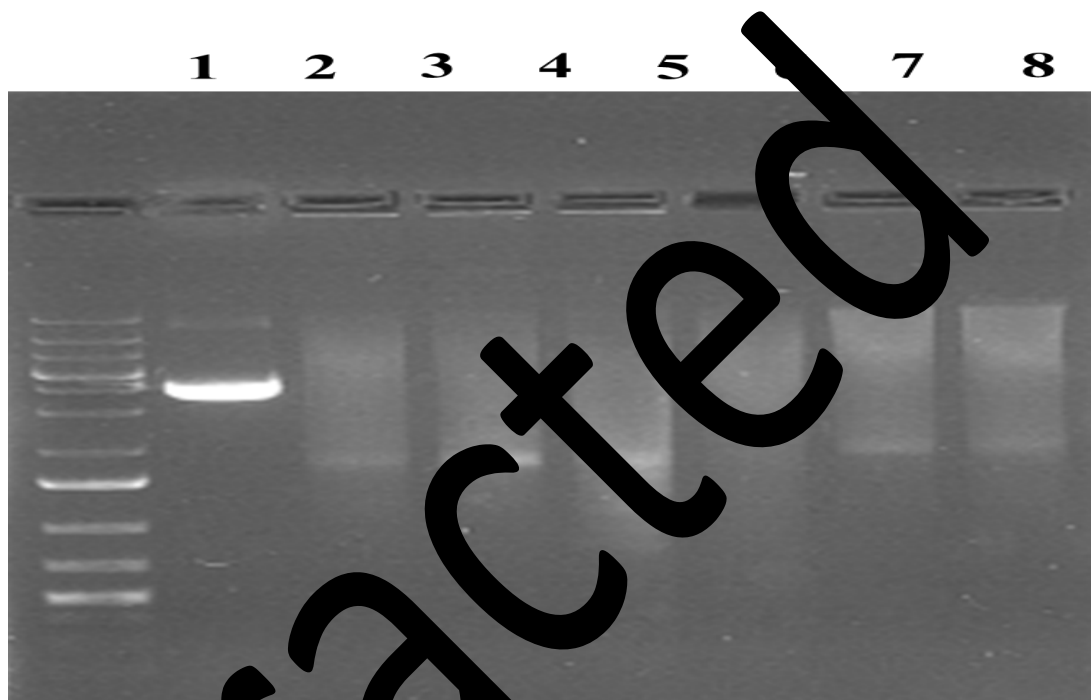
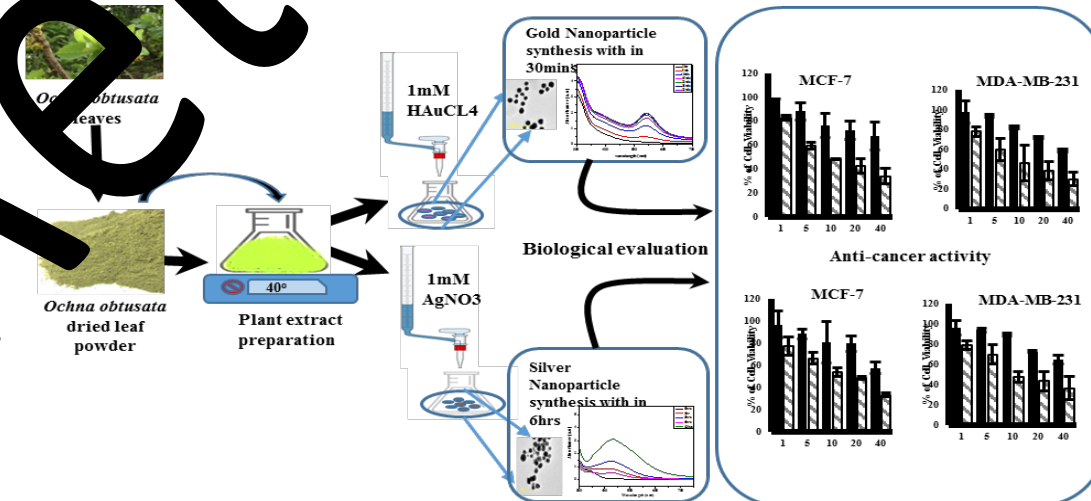


Figure 5: DNA fragmentation analysis using agarose gel electrophoresis. Lane 1- Ladder, Lane 2- control (untreated cells), Lane 3- AgNP- 5ug/ml, Lane 4- AgNP- 10ug/ml, Lane 5-AgNP- 15ug/ml, Lane 6-AuNP- 5ug/ml, Lane 7-AuNP- 10ug/ml, and Lane 8-AuNP- 15ug/ml.

Graphical abstract:



Graphical abstract: Schematic synthesis of Silver and Gold nanoparticles using *O. obtusata* aqueous leaf extract.

Acknowledgment:

The authors thank Pondicherry University for financial support. The authors are also thankful to the central instrumentation facility, Pondicherry University.

References

1 Huang Z., Jiang X., Guo D. and Gu N. 2011, Controllable synthesis and biomedical applications of silver

nanomaterials. Journal of nanoscience and nanotechnology 11, 9395-9408

2 Bharali D. J., Khalil M., Gurbuz M., Simone T. M. and Mousa S. A. 2009, Nanoparticles and cancer therapy: a concise review with emphasis on dendrimers. International journal of nanomedicine 4, 1

- 3 Yamada M., Foote M. and Prow T. W. 2015, Therapeutic gold, silver, and platinum nanoparticles. Wiley Interdisciplinary Reviews: Nanomedicine and Nanobiotechnology 7, 428-445
- 4 Das M., Shim K. H., An S. S. A. and Yi D. K. 2011, Review on gold nanoparticles and their applications. Toxicology and Environmental Health Sciences 3, 193-205
- 5 Quattrocchi U. (CRC Press/Taylor&Francis Group, 2012).
- 6 Banik B. L., Fattahi P. and Brown J. L. 2016, Polymeric nanoparticles: the future of nanomedicine. Wiley Interdisciplinary Reviews: Nanomedicine and Nanobiotechnology 8, 277-299
- 7 Jiang Y., Hong S., Mizuhata T., Dong K., Lee Y.-W., Gu S., Mooney D. J., Decher G., Liao X.-J. and Kotello V. M. 2015, The interplay of size and surface functionality on the cellular uptake of sub-10 nm gold nanoparticles. Nano 9, 9986-9993
- 8 Khan I., Saeed K. and Khan I. 2017, Nanoparticles: Properties, applications and toxicities. Arabian Journal of Chemistry
- 9 Di Pietro P. 2017, Hybrid organic-organic nanomaterials for applications at the biointerfaces.
- 10 Daraee H., Eatemadi A., Abbasi E., Fekri Aval S., Kouhi M. and Akbarzadeh A. 2016, Application of gold nanoparticles in biomedical and drug delivery. Artificial cells, nanomedicine, and biotechnology 44, 410-422
- 11 Kim D., Shin K., Kwon S. G. and Hyeon T. 2018, Synthesis and biomedical applications of multifunctional nanoparticles. Advanced Materials 30, 1802309
- 12 Kulkarni N. and Muddapur U. 2014, Biosynthesis of metal nanoparticles: a review. Journal of Nanotechnology 2014
- 13 Hyeon T. 2003, Chemical synthesis of magnetic nanoparticles. Chemical Communications 927-934
- 14 Iravani S., Korbekandi H., Mirmohammadi S. and Zolfaghari B. 2016, Synthesis of silver nanoparticles: chemical, physical and biological methods. Research in pharmaceutical sciences 9, 385
- 15 Santidos N. and Horsfall L. E. 2014, Biological synthesis of metallic nanoparticles by bacteria, fungi and plants. Journal of Nanomedicine & Nanotechnology 5, 1
- 16 Kowshik M., Ashtaputre S., Kharrazi S., Vogel W., Urban J., Kulkarni S. K. and Paknikar K. 2002, Extracellular synthesis of silver nanoparticles by a silver-tolerant yeast strain MKY3. Nanotechnology 14, 95
- 17 Heinz H., Farmer B. L., Pandey R. B., Slocik J. M., Patnaik S. S., Pachter R. and Naik R. R. 2009, Nature of molecular interactions of peptides with gold, palladium, and Pd- Au bimetal surfaces in aqueous solution. Journal of the American Chemical Society 131, 9704-9714
- 18 Kapuścińska A. and Nowak I. in *Nanobiomaterials in Galenic Formulations and Cosmetics* 395-417 (Elsevier, 2016).
- 19 Ahmed S., Ahmad M., Swami B. L. and Ikram S. 2016, A review on plants extract mediated synthesis of silver nanoparticles for antimicrobial applications: a green expertise. Journal of advanced research 7, 17-28
- 20 Guzman M., Dille J. and Godet S. 2012, Synthesis and antibacterial activity of silver nanoparticles against gram-positive and gram-negative bacteria. Nanomedicine: Nanotechnology, biology and medicine 8, 37-45
- 21 Srikar S. K., Giri D. D., Pal D. B., Mishra P. K. and Upadhyay S. N. 2016, Green synthesis of silver nanoparticles: a review. Green and Sustainable Chemistry 6, 34

- 22 Narayanan K. B. and Sakthivel N. 2010, Biological synthesis of metal nanoparticles by microbes. *Advances in colloid and interface science* 156, 1-13
- 23 Abadi M. n., Agarwal A., Barham P., Brevdo E., Chen Z., Citro C., Corrado G. S., Davis A., Dean J. and Devin M. 2016, others: TensorFlow: Large-Scale Machine Learning on Heterogeneous Distributed Systems. *arXiv preprint*
- 24 Chen S., Wei Y., Yuan X., Lin J. and Liu L. 2016, A highly stretchable strain sensor based on a graphene/silver nanoparticle synergic conductive network in a sandwich structure. *Journal of Materials Chemistry C* 4, 4304-4311
- 25 Wei L., Lu J., Xu H., Patel A., Chen Z.-S. and Chen G. 2015, Silver nanoparticles: synthesis, properties, and therapeutic applications. *Drug discovery today* 20, 555-601
- 26 Patra S., Mukherjee S., Barui A. K., Ghoshuly A., Ghose S. and Patra C. R. 2015, Green synthesis, characterization of gold and silver nanoparticles and their potential application for cancer therapeutics. *Materials Science and Engineering: C* 53, 298-309
- 27 Carabineiro S., Thavorn-Amornsri T., Pereira M., Serp P. and Figueiredo J. 2012, Comparison between activated carbon, carbon xerogel and carbon nanotubes for the adsorption of the antibiotic ciprofloxacin. *Catalysis Today* 186, 29-34
- 28 Boisselier E. and Astruc D. 2009, Gold nanoparticles in nanomedicine: preparations, imaging, diagnostics, therapies and toxicity. *Chemical society reviews* 38, 1759-1782
- 29 Carabineiro S. A. C. and Thompson D. T. 2010, Gold catalysis. *Gold: Science and applications*, 89-122
- 30 Parveen K., Banse V. and Ledwani L. in *AIP Conference Proceedings*. 020048 (AIP Publishing).
- 31 Mohan N. A. N., Arham N. A., Jai J. and Haq A. in *Advanced Materials Research* 150-355 (Trans Tech Publ).
- 32 Menon R., Rajeshkumar S. and Kumar V. 2018, A review on biogenic synthesis of gold nanoparticles, characterization, its applications. *Resource-Efficient Technologies*
- 33 Parveen K., Sreeramulu K., Venkata Rao G., Gunasekar D., Martin M. and Bodo B. 1997, Two new biflavonoids from *Ochna obtusata*. *Journal of natural products* 60, 632-634
- 34 Dandi A. K. R., Lee D. U., Tih R. G., Gunasekar D. and Bodo B. 2012, Phytochemical and biological studies of *Ochna* species. *Chemistry & biodiversity* 9, 251-271
- 35 Karthigeyan K., Kumaraswamy I. and Arisdason W. 2013, An assessment of angiosperm diversity of Adyar estuary, Chennai—a highly degraded estuarian ecosystem, Tamil Nadu, India. *Check List* 9, 920-940
- 36 Karimulla S. and Kumar B. P. 2012, Evaluation of anti-ulcer activity of *Ochna obtusata* in various experimental models. *International Journal of Preclinical and Pharmaceutical Research* 3, 14-19
- 37 Ndoile M. M. *Structure, Synthesis and Biological Activities of Biflavonoids Isolated from Ochna Serrulata (Hochst.) Walp, Citeseer*, (2012).
- 38 Banavath H. N., Allam S. R., Valathati S. S., Sharan A. and Rajasekaran B. 2018, Femtosecond laser pulse assisted photoporation for drug delivery in Chronic myelogenous leukemia cells. *Journal of Photochemistry and Photobiology B: Biology* 187, 35-40
- 39 Elmore S. 2007, Apoptosis: a review of programmed cell death. *Toxicologic pathology* 35, 495-516
- 40 Hackenberg S., Scherzed A., Kessler M., Hummel S., Technau A., Froelich K., Ginzkey C., Koehler C., Hagen R. and Kleinsasser N. 2011, Silver

- nanoparticles: evaluation of DNA damage, toxicity and functional impairment in human mesenchymal stem cells. *Toxicology letters* 201, 27-33
- 41 Cao Y., Jin R. and Mirkin C. A. 2001, DNA-modified core-shell Ag/Au nanoparticles. *Journal of the American Chemical Society* 123, 7961-7962
- 42 Amendola V., Bakr O. M. and Stellacci F. 2010, A study of the surface plasmon resonance of silver nanoparticles by the discrete dipole approximation method: effect of shape, size, structure, and assembly. *Plasmonics* 5, 85-97
- 43 Liu Z., Zu Y., Fu J., Meng R., Gu S., Xing Z. and Tan J. 2010, Hydrothermal synthesis of histidine-functionalized single-crystalline gold nanoparticles and their photoluminescent absorption characteristic. *Colloids and Interfaces B: Biointerfaces* 76, 311-316
- 44 Huber A., Purdey M., Schartner E., Follis C., van der Hoek B., Giles D., Alami A., Monro T. and Ebendorff-Heidepriem H. 2016, Detection of gold nanoparticles with different sizes by absorption and fluorescence based method. *Sensors and Actuators B: Chemical* 227, 117-127
- 45 Danaei M., Dehghankhold M., Ataei S., Hasanzadeh Davarani F., Javanmard R., Dokhani A., Khorasani S. and Mozafari M. 2018, Impact of particle size and polydispersity index on the clinical applications of lipidic nanocarrier systems. *Pharmaceutics* 10, 57
- 46 Saraswathi V. S., Kamarudheen N., BhaskaraRao K. and Santhakumar K. 2017, Phytoremediation of dyes using *Lagerstroemia speciosa* mediated silver nanoparticles and its biofilm activity against clinical strains *Pseudomonas aeruginosa*. *Journal of Photochemistry and Photobiology B: Biology* 168, 107-116
- 47 Trovato M., Monforte M., Forestieri A. and Pizzimenti F. 2000, In vitro anti-mycobacterial activity of some medicinal plants containing flavonoids. *Bollettino chimico farmaceutico* 139, 221-227
- 48 Lu Y., Yang J.-x., Yang J., Lim A., Wang J. and Lee J.-P. 2009, One-pot synthesis of fluorescent carbon nanoribbon nanoparticles, and graphene by the exfoliation of graphite in ionic liquids. *ACS nano* 3, 2367-2375
- 49 Anand N. *Isolation and Identification of Microfungi from Ariyankuppam Mangrove Soil and their Application as Nanomaterials*, Department of Botany, KMCPGS, Pondicherry University, (2016).
- 50 Krishnaraj C., Muthukumar P., Ramachandran R., Balakumaran M. and Kalaichelvan P. 2014, *Acalypha indica* Linn: biogenic synthesis of silver and gold nanoparticles and their cytotoxic effects against MDA-MB-231, human breast cancer cells. *Biotechnology Reports* 4, 42-49
- 51 Lalitha P. 2015, Apoptotic efficacy of biogenic silver nanoparticles on human breast cancer MCF-7 cell lines. *Progress in biomaterials* 4, 113-121
- 52 Sivaraj R., Rahman P. K., Rajiv P., Narendhran S. and Venckatesh R. 2014, Biosynthesis and characterization of *Acalypha indica* mediated copper oxide nanoparticles and evaluation of its antimicrobial and anticancer activity. *Spectrochimica Acta Part A: Molecular and Biomolecular Spectroscopy* 129, 255-258
- 53 Prabhu D., Arulvasu C., Babu G., Manikandan R. and Srinivasan P. 2013, Biologically synthesized green silver nanoparticles from leaf extract of *Vitex negundo* L. induce growth-inhibitory effect on human colon cancer cell line HCT15. *Process Biochemistry* 48, 317-324